



## Protein adsorption–desorption on electrospray capillary walls – No influence on aggregate distribution

Suvajyoti Guha<sup>a,b</sup>, Joshua R. Wayment<sup>b</sup>, Mingdong Li<sup>a,b</sup>, Michael J. Tarlov<sup>b</sup>, Michael R. Zachariah<sup>a,b,\*</sup>

<sup>a</sup> Departments of Mechanical Engineering, Chemistry and Biochemistry, University of Maryland, College Park, MD 20742, United States

<sup>b</sup> National Institute of Standards and Technology, Gaithersburg, MD 20899, United States

### ARTICLE INFO

#### Article history:

Received 4 January 2012

Accepted 20 March 2012

Available online 28 March 2012

#### Keywords:

Electrospray

Differential mobility analysis

Immunoglobulin

Adsorption

Capillary

Passivation

Aggregates

### ABSTRACT

Adsorbed proteins on walls of glass capillaries used for electrospray (ES) can desorb and potentially affect size distributions and, thus, quantification of aggregates of proteins. In this study we use differential mobility analysis (DMA) to investigate the size distribution of various proteins eluting from bare and passivated glass capillaries. We found no significant differences in aggregate distributions from unpassivated capillaries at 'steady state' when compared to aggregate distributions from passivated capillaries implying that desorbing proteins do not influence protein aggregate distribution. Surface passivation with gelatin was found to be considerably more effective in limiting adsorption of two antibodies (Rituxan and polyclonal human IgG) compared to passivation with BSA. Gelatin passivation was also found to be stable for a few days and from a pH range of 4.8–9.0.

© 2012 Published by Elsevier Inc.

### 1. Introduction

In the past decade, the use of electrospray (ES) in conjunction with ion mobility techniques, such as differential mobility analysis (DMA) for characterization of proteins has received increased attention [1–8]. ES-DMA operates at atmospheric conditions and characterizes particles (proteins in this context), electrosprayed from solution, based on a balance of drag and electrical force [9]. The aerosol stream emanating from the ES source undergoes solvent evaporation leaving dry analyte particles which are charged to a known value using a Po-210 radioactive source [10]. The positively charged dry particles are separated within the DMA on the basis of their electrical mobility, which is inversely proportional to the projected area of the particles. At fixed voltage a specific mobility size exits the DMA and is counted with a condensation particle counter (CPC) [11]. A more detailed discussion of the technique is available elsewhere [2,12]. By scanning the DMA voltage a number versus size distribution can be obtained.

Because mobility can be related to size, ES-DMA can be used to characterize protein oligomers [1,4]. One potentially confounding effect in accurately measuring the size distribution of protein oligomers by ES-DMA is the adsorption of the protein to the bare silica

\* Corresponding author. Address: 2125 Glenn L. Martin Hall, Building 088, University of Maryland, College Park, MD 20742, United States. Fax: +1 301 314 9477.

E-mail address: mrz@umd.edu (M.R. Zachariah).

capillary. In recent work measuring size distributions of IgG proteins, we found compelling evidence for adsorption of these proteins to the glass capillary wall [4,5]. To minimize these effects we conducted measurements of protein size distributions only after the adsorption–desorption process had reached steady-state. However, in these studies, we assumed that the proteins desorbing from the capillary walls did not influence the size distributions. Recent evidence suggests that proteins adsorbed to surfaces aggregate [13–15]. Since these aggregated proteins may then desorb, one might reasonably wonder, how these desorbing proteins may impact size distributions obtained with ES-DMA, an aspect that has never been studied before.

To understand the effect of adsorbed proteins that desorb, we take the following approach: experiment I, involves obtaining size distributions of a protein, denoted A, as a function of time until the measured protein monomer signal reaches steady state (which is reached once the surface is saturated with protein A). In experiment II, another protein, denoted B, is used as a blocking agent for passivating a fresh silica capillary until surface saturation. In this case, the size distribution of protein B is obtained again as a function of time as in experiment I. The amount of protein B adsorbed on the surface can be estimated from the time taken for protein B's size distributions to reach steady state and by correlating the gas phase counts obtained with the known liquid phase concentration of this protein at steady state. This determination is described in greater details elsewhere [16] and is briefly discussed in Section 3.2. In experiment III, protein A is electrosprayed

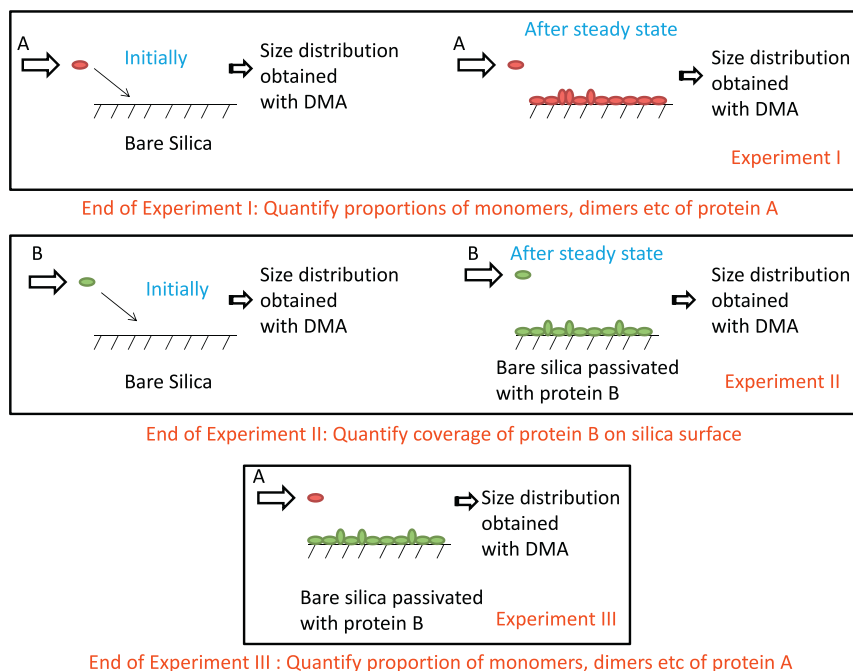


**Fig. 1.** In experiment I steady state size distribution of protein A and oligomers proportions are obtained with a bare capillary. In experiment II a different capillary is passivated with protein B. In experiment III, the size distribution of A is obtained from capillary passivated with B. The proportion of monomers and aggregates obtained from experiment III would then be compared with experiment I.

through the capillary passivated with B and size distribution of A and its oligomers are measured and compared to results of the bare capillary (experiment I).

In this paper, the size distributions of four different proteins, bovine serum albumin (BSA), polyclonal human immunoglobulin (IgG), monoclonal human immunoglobulin (RmAb), bovine immunoglobulin M (IgM) are obtained with ES-DMA using bare and passivated capillaries thus allowing a systematic comparison of the effect of capillary passivation on the quantification of monomers and aggregates of proteins. For surface passivation we use BSA [17–21] and gelatin [22,23], as blocking agents, each of which can form monolayers or multiple layers on a surface and hence reduce surface adsorption of other proteins.

## 2. Experimental section

### 2.1. Materials and sample preparation

Twenty mmol/L ammonium acetate buffer solutions were prepared by adding 0.77 g of ammonium acetate powder (Sigma Aldrich, St. Louis, MO, #631-61-8) to 0.5 L of de-ionized water (18 M $\Omega$ /cm, Barnstead nanopure UV system). The pH was adjusted to the desired values using either glacial acetic acid (Mallinckrodt, Phillipsburg, NJ, #2504-14) or ammonium hydroxide (Baker, Phillipsburg, NJ, #9721-01). The buffer at pH 2.1 was prepared by mixing 1 mL of glacial acetic acid with 3 mL of de-ionized water.

Stock gelatin (KNOX, trade name: Gelatine, # 0-41000-03500-5) solutions were prepared by suspending 1–1.5 mg in 1–1.5 mL of 20 mmol/L ammonium acetate at the desired pH in low protein binding vials (Eppendorf). The 1 mg/mL solution was heated to  $\approx 50^\circ\text{C}$  for  $\approx 5$  min for dissolution. The samples were then diluted to 0.1 mg/mL and used to passivate the capillaries. Solutions of gelatin were prepared fresh each time the capillaries were passivated.

RmAb was purified using protein A affinity column and stored at  $-18^\circ\text{C}$  in 25 mmol/L Tris buffer at pH 7.4 and  $\text{NaN}_3$  was added as a preservative. To desalt the protein sample a centrifuge filter

(30 kDa molecular weight cut off) was used immediately prior to ES-DMA analysis at 13,200 rpm for 12 min. The concentration of RmAb in 20 mmol/L ammonium acetate at pH 7 was diluted to 1 mg/mL as verified by UV-Vis measurements and the solution was further diluted to a concentration of 0.1 mg/mL. Human IgG (Sigma Aldrich, St. Louis, MO, # I4506) was prepared by suspending 1–1.5 mg in 1–1.5 mL of buffer (20 mM ammonium acetate at pH 7 in low protein binding vials).

Bovine IgM (Sigma Aldrich, St. Louis, MO, 078K4779) obtained in concentrations of 1 mg/mL was desalted as described for RmAb and diluted  $10\times$  to a concentration of 0.1 mg/mL for use in the ES-DMA.

### 2.2. Capillary surface preparation

Prior to electrospray of protein samples, 0.5–1.0 mmol/L  $\text{H}_2\text{SO}_4$ , deionized (18 M $\Omega$ /cm) ultrapure water and 20 mmol/L ammonium acetate buffer solutions were eluted sequentially for 20–30 min through the 25  $\mu\text{m}$  fused silica capillaries (TSI Inc.).

The capillaries referred to as unpassivated or bare are those that did not undergo any surface treatment before use. Passivated capillaries are those that underwent surface treatment with gelatin or BSA.

### 2.3. Electrospray-differential mobility analysis (ES-DMA)

An electrospray (TSI, Inc., Shore View, MN, #3480) source was used for aerosolizing protein solutions suspended in 20 mmol/L ammonium acetate at pH 7.0. The samples were placed in 1.5 mL vials in a pressurized chamber and then delivered to a capillary (25  $\mu\text{m}$  inner diameter, 24 cm in length, TSI Inc.). The resulting electrosprayed proteins were exposed to a Po-210 source such that proteins carried either a +1, 0 or  $-1$  charge. A negative voltage was applied at the DMA (TSI, Inc., #3080) such that the +1 charged protein would pass through the DMA to the CPC (TSI, Inc., #3025A) which then measured the gas phase concentration.

The ES was operated at an ostensibly time invariant “Taylor cone” mode [24], with a liquid flow rate of 66 nL/min, an aerosol

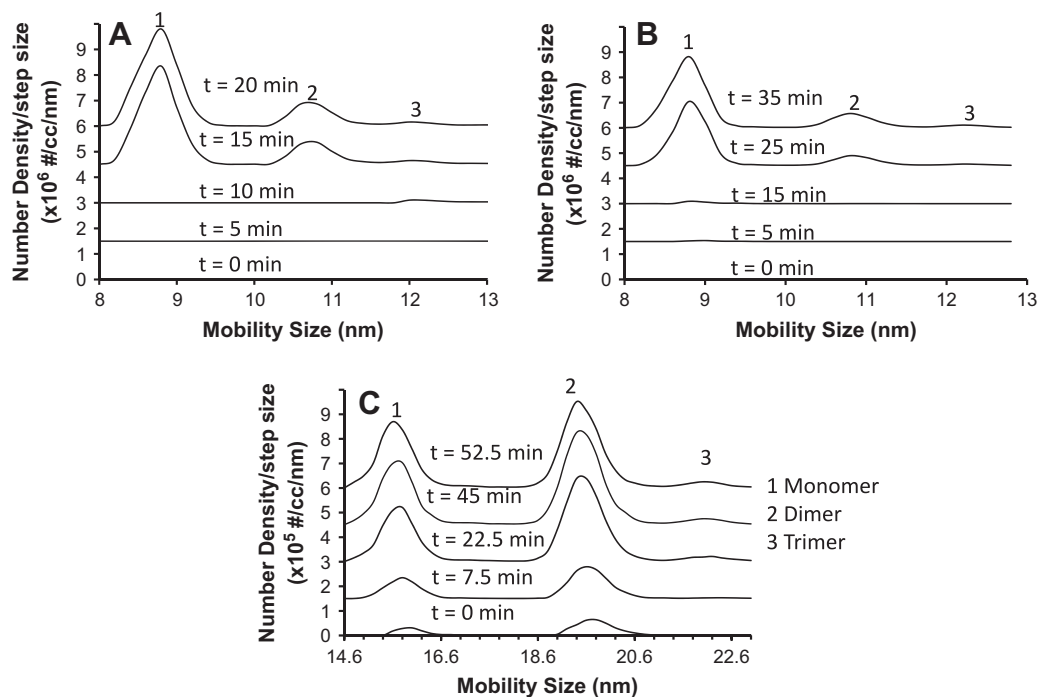


**Fig. 2.** Size distribution of RmAb (3A), IgG (3B) and IgM (3C) obtained on unpassivated capillaries. The monomer, dimer and trimer peaks for each protein are identified and labeled 1, 2 and 3 respectively based on well-established empirical correlations in between molecular weight and mobility size [1]. For clarity, the number density/step size in Fig. 3A and B have been offset by  $1.5 \times 10^6$  (#/cc/nm) for each plotted time point. For clarity, the number density/step size in Fig. 3C has been offset by  $1.5 \times 10^5$  (#/cc/nm) for each plotted time point.

flow rate of 1.2 L/min, comprising 1 L/min of air and 0.2 L/min of CO<sub>2</sub>. The DMA was operated with a sheath flow 30 L/min and the CPC was operated at a high flow mode of 1.5 L/min. Under these conditions the uncertainty in size is  $\approx 0.3$  nm [25,26].

Sixty nm polystyrene latex beads (NIST SRMs<sup>®</sup> 1964) were used to calibrate the ES-DMA system and mean mobility size was determined to be 59.4 nm consistent with previous findings [27].

The total monomer, dimer and trimer counts of the proteins were obtained by integrating the size distributions from 8 nm to 9.4 nm, 9.6 nm to 11.4 nm, 11.6 nm to 12.8 nm for RmAb and IgG, 6 nm to 7.6 nm, 8 nm to 9.2 nm and from 9.4 nm to 10.2 nm for BSA, and 14.4 nm to 16.4 nm, 18.2 nm to 20.4 nm and 20.6 nm to 22.8 nm for IgM.

Upon insertion of the different samples into the ES, we would wait about 4 min before starting to collect the data, since it would take a finite amount of time for any sample to traverse the full length of the capillary, different tubings and the DMA to eventually reach the CPC. Thus in Section 3.1, time  $t = 0$  min refers to 4 min after sample insertion.

### 3. Results and discussion

#### 3.1. Adsorption of proteins onto fused silica surface of ES

We first present results corresponding to experiment I of Fig. 1. In the data presented in Fig. 2, we see evidence for protein adsorption. To reduce the data acquisition time, the size range of scans were tailored for each protein (6–11.8 nm; BSA, 8–13.8 nm; RmAb and IgG, and 14.6–22.8 nm; IgM). Because data were collected at a step size of 0.2 nm, and dwell time of 10 s, the total scan time for BSA was 250 s, 290 s for RmAb and IgG, and 840 s for IgM.

We begin by showing the size distribution for RmAb in Fig. 2A. No counts are observed for the first 10 min, after which a rapid “breakthrough” occurs at  $t = 15$  min and three peaks at 8.8 nm, 10.6 nm and 12.2 nm are observed. Based on an empirical correla-

tion developed by Bacher et al. [1] for ES-DMA that relates molecular weight of proteins with their mobility size the peak at 8.8 nm is assigned to RmAb monomers, 10.6 nm to dimers, and 12.2 nm to trimers, in conjunction with our previous studies [28,29]. For all subsequent times the size distribution of monomers, dimers and trimers are invariant. For IgG we also see a similar trend as shown in Fig. 2B. Initially there are no detectable counts, but at  $\approx 25$  min a sudden increase in counts occurs until steady state is achieved at 35 min. For clarity, other time points are omitted.

For IgM we see a slightly different trend as evident in Fig. 2C. The monomers and dimers are detected immediately, and gradually increase until steady state is reached at  $\approx 52$  min<sup>1</sup>. The near immediate appearance of IgM suggests that its affinity for the silica capillary wall is much lower relative to RmAb and IgG.

The proportion of monomers, dimers and trimers are quantifiable from Fig. 2 but are discussed later in Section 3.4.

#### 3.2. Adsorption of BSA to passivate capillaries

Sections 3.2 and 3.3 describe results corresponding to experiment II of Fig. 1, where BSA and gelatin are used to passivate the capillary surface.

BSA has been widely used as a blocking agent to limit non-specific adsorption of proteins [17–21]. In this section, we describe the protocol for passivating the ES capillaries with BSA at pH conditions close to its isoelectric point (pI) of 4.8 [30]. At neutral conditions we do not observe significant variation in the size

<sup>1</sup> It should be pointed out that the time taken for different proteins to attain steady state is a function of the properties of the protein, the solute and the concentration of the protein. For monolayer adsorption we have found the time for steady state to be inversely proportional to the concentration [16]. However, based on our experience, protein adsorption can often be multilayered with the number of layers being protein dependent. This precludes us from developing any predictive models for the time taken by different proteins to reach steady state.

distribution as a function of time using the ES-DMA implying little adsorption.

ES-DMA offers the opportunity to quantify the amount of BSA adsorbed as described below. We have observed that proteins exhibit a time dependent signal that increases monotonically and eventually reaches steady state. At steady state, assuming 100% recovery of protein (i.e., all protein molecules entering the capillary exit the capillary), the gas phase counts of the protein obtained using the ES-DMA can be correlated to the concentration of protein in solution. By using the time-dependent behavior observed before steady-state, the amount adsorbed as a function of time can then be estimated. Further, knowing the capillary surface area, the surface coverage of any protein can be quantified. A detailed discussion for the determination of surface coverage can be found elsewhere [16]. As in our previous work, time is expressed in equivalent capillary volume which is defined as the product of time and capillary flow rate, normalized by total internal volume of the capillary.

For BSA passivation,  $\approx 0.05$  mg/mL of BSA at pH 4.8 is electro-sprayed for 1 h (or approximately 32 capillary volumes) through a new capillary after its surface has been cleaned following the procedure outlined in Section 2.2. In Fig. 3A, no elution from the capillary is observed for the first 16 capillary volumes, after which the monomer and dimer counts increase monotonically and reach steady state at  $\approx 27$  capillary volumes. After about 60 min (32 capillary volumes) the protein sample is replaced with 20 mmol/L ammonium acetate at pH 7.0 and the capillary flushed using this buffer while simultaneously monitoring the size distribution. Fig. 3B display mobility spectra during the flushing phase showing that the mobility size of monomers and dimers remains unchanged and that there is a monotonic decrease in the number density of desorbing monomers and dimers.

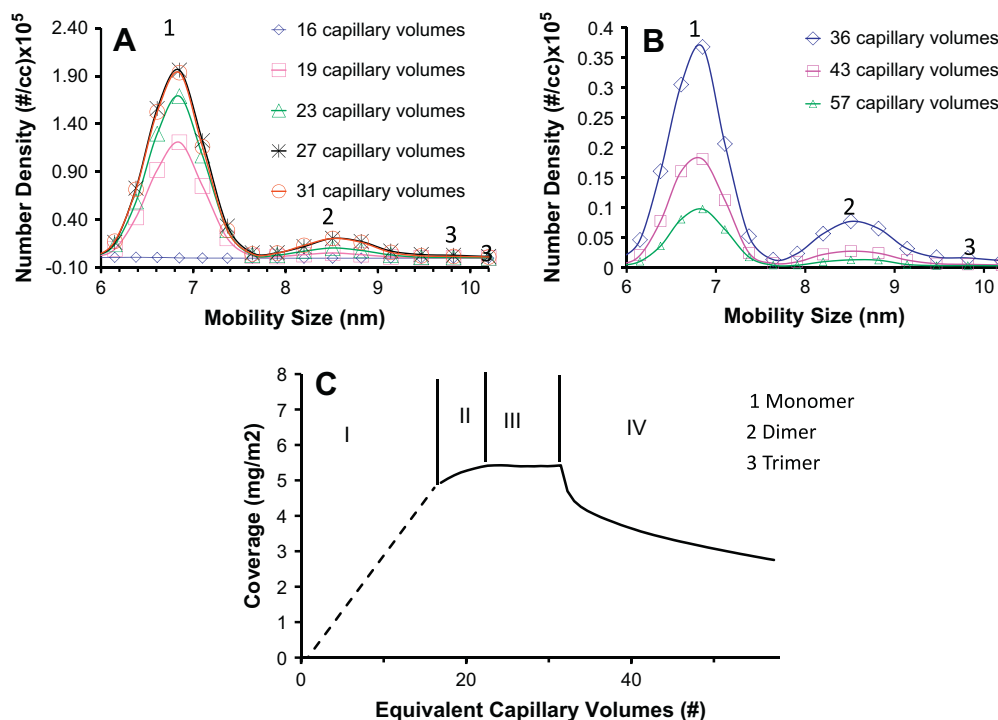


**Fig. 3.** (A) Size distributions of monomers, dimers, and traces of trimers (not evident from this figure) of BSA eluting through the capillary as a function of capillary volumes. The Y-axis has been offset slightly to show that BSA is not eluting at 16 capillary volumes. (B) Size distribution of the desorbing species as a function of capillary volumes when the protein sample is replaced with buffer. (C) Coverage of BSA adsorbed and desorbed as a function of capillary volumes (refer text for details). The dotted line represents when no protein is eluting. The monomer, dimer and trimer peaks for each protein are assigned and labeled 1, 2 and 3, respectively, based on well-established empirical correlations between molecular weight and mobility size [1]. Refer to the text for a discussion of the domains I, II, III and IV.

Fig. 3C shows the resulting calculated coverage of the BSA as a function of time. Region I in Fig. 3C, corresponds to when there is no protein eluting, (represented by the dotted line), region II corresponds to when the protein is first observed eluting, and the concentration continues to increase, region III corresponds to steady state, and region IV corresponds to when the protein is replaced with the pH 7.0 buffer.

The calculated coverage at steady state is determined to be  $5.4$  mg/m<sup>2</sup> (region III). Prior work on BSA adsorbed to different nanoparticles report coverages ranging from  $1.2$  mg/m<sup>2</sup> to  $6$  mg/m<sup>2</sup> under a variety of conditions [32–36] using UV based spectroscopy. As discussed in our prior work [16], protein coverage can be a function of concentration, ionic strength, pH, surface type, solution type, and flow conditions, thus it is not surprising to find such a wide range of coverage in literature. Almost all prior studies with BSA were conducted using non-volatile buffers (for e.g., phosphate buffer [33,34]) and at very high concentrations (of the order of mg/ml [33]). The ES-DMA cannot be operated under similar conditions primarily because of the ES itself (as non-volatile salts interfere with protein signal and high concentrations create “droplet induced aggregates” [28] or may clog ES capillaries), thus a direct comparison with literature is not possible. Nevertheless, as our results are within the reported range in literature [32–36] and further because prior studies were conducted on proteins at stagnant conditions, it implies that BSA adsorption is neither influenced by shear nor by surface curvature.

Assuming that BSA is spherical and using the measured diameter of  $6.6$  nm obtained by the ES-DMA, the theoretical coverage of a monolayer is  $3.2$  mg/m<sup>2</sup> (calculations shown in Appendix A.1). Electrostatic repulsion between the protein molecules might reduce the actual coverage required to form a monolayer. Further, as soft proteins like BSA may considerably change conformation

upon adsorption to silica, as has been found on several occasions [34–36], they might promote multilayered adsorption. Such a multilayered adsorption scheme can be qualitatively explained as follows [31]: first a layer of protein adsorbs to the surface and denatures, this promotes the exposure of hydrophobic residues of the first layer of protein which then attracts a second layer of protein; as the layers build on top of each other, the interaction in between successive upper layers progressively weaken (as the extent of denaturation and exposure of hydrophobic residues are reduced) and thus protein adsorption eventually stops. Given, that the coverage for BSA on ES silica surface obtained with ES-DMA is above the theoretical coverage, it is reasonable to infer that the adsorption is indeed multilayered.

After  $\approx 30$  capillary volumes of flushing, the amount of BSA remaining on the surface is estimated to be  $\approx 2.8$  mg/m<sup>2</sup>, which is close to the theoretical coverage of 3.2 mg/m<sup>2</sup> for a monolayer. This also implies that approximately 50% of the BSA desorbs from the silica surface which is higher than the amount of RmAb desorption previously quantified with ES-DMA [16]. In the previous work the coverage of RmAb to ES silica surface was approximately equal to a theoretical monolayer and thus lesser than the multilayered coverage obtained for BSA in this work. This signifies that the top-most layer of BSA is loosely bound to silica and hence comes off easily during desorption.

### 3.3. Adsorption of gelatin to passivate capillaries

In this section gelatin adsorption is quantified using ES-DMA. The use of gelatin layers to passivate surfaces against protein adsorption has been previously reported [22]. In our case, gelatin was deposited on glass capillary surfaces by electrospraying  $\approx 31$  capillary volumes of a gelatin solution through a freshly prepared capillary. The passivation process was also assessed using the DMA. Fig. 4A shows the mobility distribution as a function of capillary volumes during the passivation. The size distributions are clearly wider than for the other proteins in this paper, and reflect the heterogeneity of gelatin.

As described above for BSA, we can estimate the surface coverage of gelatin by monitoring the time course evolution of the gelatin signal. Fig. 4B plots the experimentally determined surface coverage as a function of capillary volume for a gelatin solution concentration of 0.1 mg/ml. Little gelatin is observed initially (up to 5 capillary volumes). Then the gelatin signal gradually increases and eventually reaches steady state (5–20 capillary volumes), after which there is no significant variation in the size distribution (within experimental variability) as shown in Fig. 4A. At steady state the gelatin surface coverage is estimated to be 4.2 mg/m<sup>2</sup>. This value is within the widely varying coverage of  $\approx 1$  mg/m<sup>2</sup> to  $\approx 9$  mg/m<sup>2</sup>

obtained for gelatin using surface force apparatus, spectrophotometry, fluorescent spectroscopy, ellipsometry and small-angle neutron scattering on flat surfaces and nanoparticles [37–41]. As mentioned in the previous section, it is reasonable to find such an order of magnitude variation in coverage especially because the surface type, buffer and the analytical technique used are different.

If we consider the peak mobility of gelatin to be 7 nm (see Fig. 4A), and assuming the protein to be an equivalent sphere, the theoretical maximum surface coverage is  $\approx 3.2$  mg/m<sup>2</sup> (calculations shown in Appendix A1). It should be pointed out that such an assumption is approximate especially given the heterogeneity of the sample. As the protein size can widely vary from 4 nm to 16 nm (implying the molecular weight would also vary drastically, [1]) the coverage can vary too, thus making a definitive assignment of what constitutes a theoretical monolayer coverage difficult. Using dynamic light scattering [41] it has been inferred that even for coverages as low as 1–2 mg/m<sup>2</sup>, gelatin can form multiple layers. Given that our experimentally determined coverage is more ( $\approx 4.2$  mg/m<sup>2</sup>) it is likely that gelatin adsorbs to form multiple layers on ES silica surface. Also, comparing our experiments conducted at high shear [16] with all previous studies conducted at stagnant conditions [37–41] it is evident that the gelatin coverage is not affected by shear, in conjunction with results obtained with BSA in the previous section.

An interesting feature of gelatin adsorption is that it appears to be largely irreversible, because little desorption is observed over a wide range of flushing conditions (pH 4.8 to pH 9.0) (data not shown). It has been suggested that gelatin's strong interaction with surfaces may be due to its ability to form a gel at room temperature by physical entanglement [42]. This behavior is in contrast to the other proteins examined (BSA, RmAb, IgG and IgM) all of which show significant desorption from unpassivated (i.e. bare) capillaries.

### 3.4. Effect of size distribution on passivated, partially passivated and unpassivated capillaries

We find that for bare silica, i.e., for unpassivated surfaces it takes several capillary volumes (10–30) for BSA, IgG, RmAb and IgM size distributions to reach steady state (as shown in Fig. 2, where time is expressed in minutes). When a capillary is passivated with BSA the number of capillary volumes to reach steady state is reduced for IgG, RmAb and IgM (5–20 capillary volumes). Although passivation by BSA reduces adsorption of these proteins, some nonspecific adsorption still occurs suggesting protein adsorption to the pre-adsorbed BSA layer thus a BSA passivated capillary will act as a partially passivated surface for IgG, RmAb and IgM. This is in disagreement with previous findings conducted

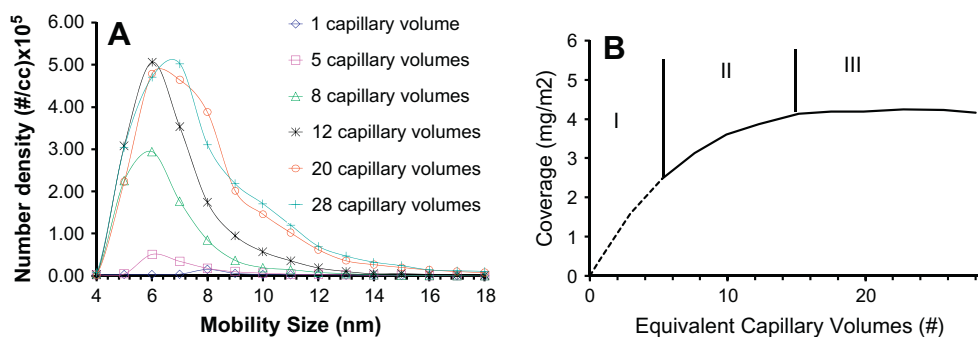


**Fig. 4.** (A) Mobility distribution of 0.10 mg/mL gelatin in 20 mmol/L ammonium acetate at pH7. (B) The coverage of gelatin on fused silica as a function of time. Dotted line represents when no or small amounts of protein eluting. Domain I corresponds to when no or little gelatin eluting, domain II corresponds to increase in concentration of gelatin eluting and domain III corresponds to steady state.

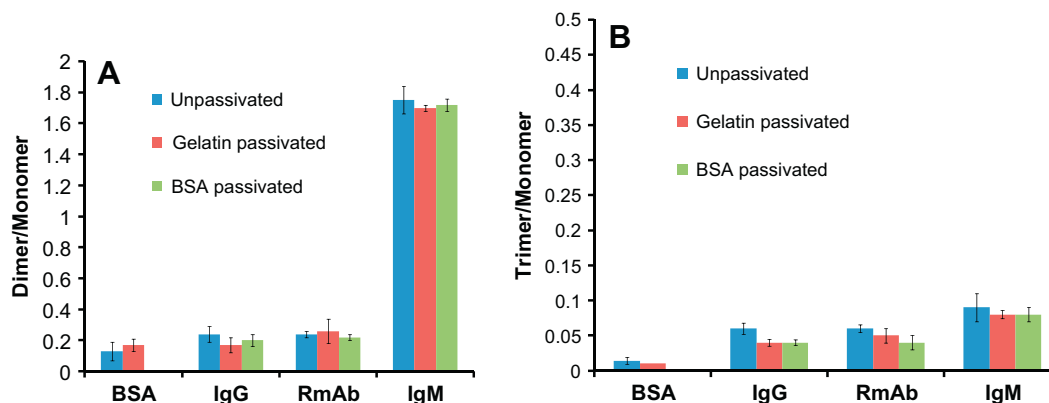


**Fig. 5.** Dimer to monomer (5A) and trimer to monomer ratios (5B) of four different proteins on unpassivated, gelatin passivated and BSA passivated surfaces. The uncertainties are from measurements made in triplicates.

with Fourier transform infrared spectroscopy where BSA adsorbed to hydrophilic surface was monolayered and was also found to be effective against different proteins including IgGs [17].

In contrast, for a capillary passivated with gelatin, we observe that IgG and RmAb size distributions reach steady state immediately, while BSA and IgM take time before reaching steady state (5–10 capillary volumes). Therefore, we conclude that the gelatin passivated capillary nearly completely prevents nonspecific adsorption of IgG and RmAb, while less so for BSA and IgM, i.e. a gelatin passivated capillary is a completely passivated surface for IgG and RmAb and a partially passivated surface for BSA and IgM. Size distributions of RmAb, IgG, BSA and IgM on unpassivated and passivated surfaces after steady state are provided in Appendix A2 (Fig. A1).

Because we have steady state size distributions of RmAb, IgG, IgM and BSA for unpassivated and gelatin passivated capillaries, and RmAb, IgG and IgM size distributions for a BSA passivated capillary, we can assess the effect of capillary passivation on size distributions, i.e. we are in a position to compare size distributions obtained in experiment I (Fig. 1) with those obtained in experiment III (Fig. 1). Fig. 5 plots dimer/monomer and trimer/monomer peak area ratios for steady state conditions for unpassivated, BSA passivated, and gel passivated capillaries. The different surfaces appear to have no effect on the observed dimer/monomer and trimer/monomer ratio. Thus, we conclude that for the proteins and the capillary surface passivation conditions examined here, surface passivation does not alter size distributions<sup>2</sup> measured under steady state condition relative to that obtained using a bare glass capillary (i.e. unpassivated capillary).

It should be noted that RmAb and IgG were observed to elute nearly immediately at several different concentrations from gelatin passivated capillaries implying little or no adsorption. These results indicate that protein recovery from a gelatin passivated surface is nearly  $\approx 100\%$ . With an unpassivated or partially passivated surface the eluting monomer, dimer and trimer counts of proteins at steady state are found to be equal (within experimental variability) to the respective counts from a gelatin passivated sur-

face (Appendix A2, Fig. A1) or in other words *steady state in an unpassivated surface also corresponds to equilibrium*.

We now consider several possible scenarios for why unpassivated or partially passivated capillaries do not influence the size distributions. Proteins could be desorbing either as monomers or aggregates such as dimers, and trimers, and could be desorbing in their native form or in denatured state [34,43,44]. Careful analysis of the mobility spectra between the desorption and adsorption experiments for all proteins indicate no significant mobility size change in the monomers or dimers indicating that at least to the level of our instrument resolution, 0.3 nm in mobility diameter [25,26], we are not able to discern any changes in conformation. We also found the desorbing species to be primarily monomers. This could either mean the proteins on the surface of the capillary elute as monomers or as dimers or larger aggregates that then dissociate to form monomers during passage through the capillary or the larger aggregates are irreversibly bound to the ES capillary surface and do not desorb at all. Given that the upper limit of our DMA range in its current configuration is 80 nm and that the lower limit of detection is  $10^9$  particles/mL, it is also possible that large aggregates at low concentration desorb from the surface and pass undetected as well. Irrespective of the mechanism of desorption and the sizes of the desorbing aggregates, it is evident that the desorbing proteins do not influence the aggregate distribution.

### 3.5. Efficacy of gelatin passivation in repelling different protein monomers

The strong passivating behavior of gelatin against RmAb and IgG and the limits of the time resolution of our experiment preclude us from determining if any adsorption at all is taking place; however, we can perform desorption measurements to estimate the efficacy of passivation. In these experiments, protein is flowed through the capillary until the size distribution reaches steady state and then the capillary (unpassivated and gelatin passivated) is flushed with 20 mmol/L ammonium acetate buffer at pH 7.0. The temporal data for monomer desorption are presented in Fig. 6 for both unpassivated and gelatin passivated surfaces.

It is evident from Fig. 6, that desorption of monomers observed from unpassivated capillaries is significantly higher than that seen for gelatin passivated capillaries for RmAb and IgG. As a metric, a coating efficacy parameter  $\eta$ , is defined as:

$$\eta = \frac{\text{Monomer}_{\text{unpassivated}} - \text{Monomer}_{\text{passivated}}}{\text{Monomer}_{\text{unpassivated}}} \quad (1)$$

where  $\text{Monomer}_{\text{passivated}}$  and  $\text{Monomer}_{\text{unpassivated}}$  are the desorbed total monomer counts from passivated and unpassivated capillaries at a time of when the buffer starts to elute (at 0 capillary volumes). A

<sup>2</sup> It should be pointed out that the dimer and trimers seen in these size distributions may not necessarily be intrinsic solution aggregates, as a portion of it may get created by the artificial induction of two or more monomers in the same ES droplet, which is also referred to as “droplet induced aggregation” [28]. This is especially true for RmAb and IgG as we demonstrated before [28,29]. However, in this article we are interested in systematically studying the difference in the distributions before and after passivation. If there was any difference in intrinsic aggregates because of desorbing proteins from unpassivated surfaces, then we would have also seen a difference in the observed distributions as well. The fact that we do not see any such difference in aggregate distribution of different proteins using passivated and unpassivated surfaces implies that the intrinsic solution aggregate proportions for the different proteins considered here also stay the same.

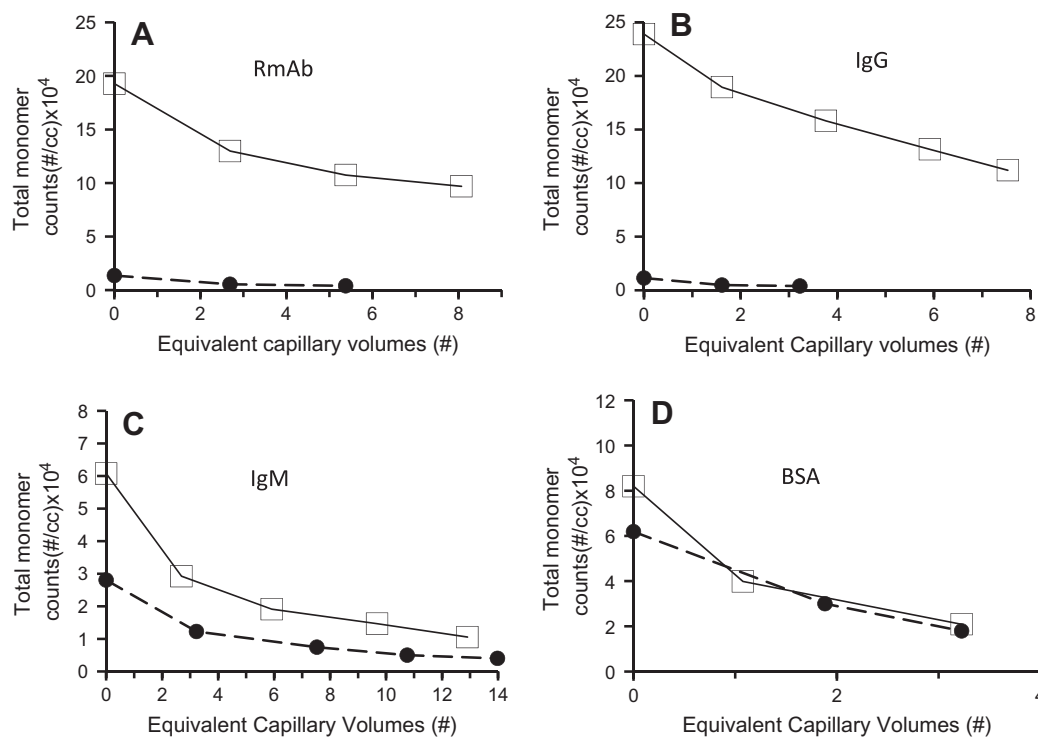


**Fig. 6.** Desorption of monomers of IgG (A), RmAb (B), BSA (C) and IgM (D) for the gelatin passivated (solid circle, dotted line) and unpassivated capillaries (open square, solid line) at pH 7.0. For Fig. 6A and B, data collection for the desorbing RmAb and IgG from gelatin passivated surfaces were stopped after approximately  $\approx 3$ –5 capillary volumes, since the amount of proteins desorbing by then was too little to be quantifiable with the ES-DMA.

**Table 1**  
Comparison of efficacy of gelatin passivation for each of proteins.

Proteins	$\eta$
BSA	0.57
IgG	0.95
RmAb	0.93
IgM	0.54

value of unity would then imply a perfectly passivating coating or proteins that are adsorbed irreversibly.

Table 1 presents the coating efficacy parameter,  $\eta$ , of gelatin for the proteins studied. The gelatin passivation seems to be especially effective in reducing adsorption of antibodies IgG and RmAb. Gelatin has an isoelectric point (pI) of 4.7–5.3 [45,46] which is close to the pI of BSA (pH 4.8). At pH 7.0, both proteins are negatively charged and yet they show a propensity to adsorb, implying that BSA's affinity towards gelatin results from hydrophobic interactions [30,47]. On the other hand, IgG (pI 6.3–9.3) and RmAb (pI 8.5) are fairly neutral or positively charged at pH 7.0, and yet, gelatin which is negatively charged at this pH, repels both the immunoglobulins, the reasons for which are not clear to us. The pI of the IgM used here is unknown, so we are unable to determine if the enhanced affinity is due to electrostatic effects or simply because IgM is  $\approx 5$  times larger than the IgG proteins and, thus, has more potential interactions sites per molecule.

### 3.6. Stability of gelatin passivation

The stability of gelatin passivation over 3 days was studied by electro spraying RmAb at 0.1 mg/mL at different times. We found that the size distribution of RmAb reached steady state almost immediately upon sample introduction, indicating that the gelatin passivation was still intact.

Buffers at pH 2.1 to pH 9.0 were flowed through the ES and size distributions obtained with ES-DMA to determine if gelatin was desorbing from gelatin passivated capillaries. No evidence of gelatin desorption was found from pH 4.8 to pH 9.0 although the passivation became unstable under acidic conditions (pH 2.1) and gelatin elution was detected by ES-DMA. Unfortunately gelatin desorption at pH 2.1 could not be quantified directly because the “Taylor cone” at the ES capillary tip was unstable at this pH for an initial period of time, which likely resulted from significant desorption of gelatin. In addition, when RmAb solution (0.1 mg/mL solution, 20 mmol/L ammonium acetate at pH 7.0) was flowed through a gelatin passivated capillary previously flushed with buffer at pH 2.1 for 1 h a significant amount of RmAb was found to adsorb with an estimated coverage of  $\approx 2.0$  mg/m<sup>2</sup>. A coverage of  $\approx 3.4$  mg/m<sup>2</sup> for RmAb on a unpassivated glass capillary surface was previously determined using ES-DMA [16]. Thus, we conclude that acid treatment leads to a capillary surface with some exposed silica that act as sites for RmAb adsorption.

## 4. Conclusions

We systematically compared size distributions obtained for passivated and unpassivated capillaries at steady state and found the size distributions to remain unchanged. Therefore, we conclude that at least for the proteins examined in this study, protein adsorption does not influence aggregate distributions measured at steady state by ES-DMA. Although, size distributions of different proteins in this study were obtained using differential mobility analyzer, our findings apply to other techniques that use ES for aerosolization of proteins as well (e.g. mass spectrometry). We also presented a simple method of passivating capillaries with BSA and gelatin and are able to quantify the coverages of these proteins onto ES capillaries in situ using the ES-DMA. Although in the ES-mass spectrometry community it is fairly common to passivate

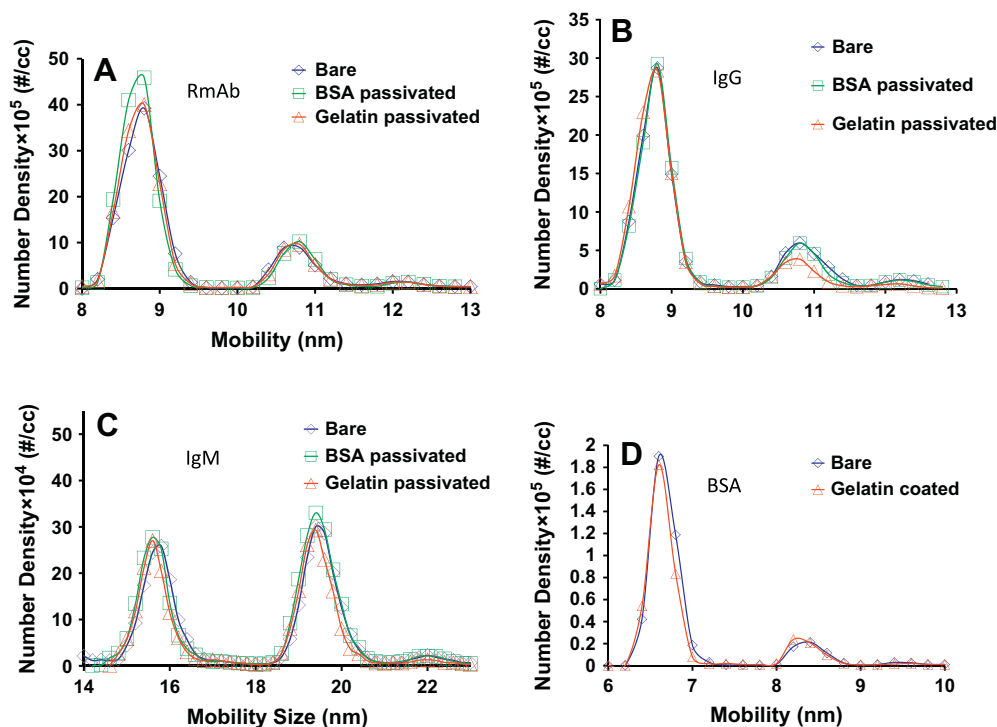


**Fig. A1.** Size distributions of RmAb (A), IgG (B), IgM (C) and BSA (D) obtained using ES-DMA on bare (open diamond, royal blue), BSA passivated (open square, green) and gelatin passivated (open triangle, red) surfaces, respectively, at steady state. The slight variations in the size distributions arise because of experimental variability. (For interpretation of the references to color in this figure legend, the reader is referred to the web version of this article.)

capillaries with polyethylene glycols (PEGs) [48] this is the first time, to the best of our knowledge, that passivation for ES-DMA has been systematically explored. We also found that gelatin passivated capillaries are effective in reducing non-specific adsorption of immunoglobulins and are stable up to about 3 days within a pH range of 4.8–9.0 although gelatin desorption was observed at low pH ( $\approx 2.1$ ). In this regard, we also attempted to PEGylate our ES capillaries (data not shown) with 5 kDa and 20 kDa silane PEGs but found gelatin to perform significantly better compared to these PEGs. In the future, the coating efficiency of gelatin (or other PEGs or proteins) against several other proteins can also be studied following our approach.

## 5. Disclaimer

Reference to commercial equipment or supplies does not imply endorsement by the University of Maryland or the National Institute of Standards and Technology.

## Appendix A

### A.1. Calculation of maximum theoretical coverage for a monolayer

The maximum possible number of proteins ( $N_{protein}$ ) that can adsorb to the ES silica surface is given by:

$$N_{protein} = \frac{\pi D_{capillary} L_{capillary}}{\pi d_{protein}^2} \quad (E1)$$

where  $D_{capillary}$  and  $L_{capillary}$  are the inner diameter and length of the capillaries respectively and  $d_{protein}$  is the mobility diameter of the protein as obtained with ES-DMA. As the DMA operates in the aerosol phase, we assume here, that the mobility diameter of the protein measured by DMA is the same as in the liquid phase. This assumption may not always be valid as the conformation of the

protein may change upon adsorption. Further, the maximum theoretical coverage ( $\Gamma$ ) can be determined by using:

$$\Gamma = \frac{N_{proteins} M_w}{\pi D_{capillary} L_{capillary} N_{av}} \quad (E2)$$

Combining E1 and E2 we get,

$$\Gamma = \frac{4M_w}{\pi d_{protein}^2 N_{av}} \quad (E3)$$

Where  $M_w$  is the molecular weight of the protein and  $N_{av}$  is the Avogadro's number. For calculating the theoretical monolayer coverage of BSA, the molecular weight used was 66 kDa and the  $d_{protein}$  used was 6.6 nm. Using this approach the theoretical coverage for BSA was determined to be 3.2 mg/m<sup>2</sup>.

The molecular weight of the gelatin was unknown and hence was determined to be 75 kDa by employing a molecular weight-mobility size correlation developed previously [1] and the  $d_{protein}$  used was 7.0 nm. This molecular weight predicted by ES-DMA is in moderate agreement with previously obtained values in literature [37,38]. Using this approach the theoretical coverage for gelatin was determined to be 3.2 mg/m<sup>2</sup>.

### A.2. Aerosol phase size distributions obtained for different proteins on different surfaces

See Fig. A1.

## References

- [1] G. Bacher, W.W. Szymanski, S.L. Kaufman, P. Zollner, D. Blaas, G. Allmaier, J. Mass Spectrom. 36 (2001) 1038–1052.
- [2] S.L. Kaufman, J.W. Skogen, F.D. Dorman, F. Zarrin, K.C. Lewis, Anal. Chem. 68 (1996) 1895–1904.
- [3] S.L. Kaufman, J. Aerosol Sci. 29 (1998) 537–552.

- [4] L.F. Pease, J.T. Elliott, D.H. Tsai, M.R. Zachariah, M.J. Tarlov, *Biotech. Bioeng.* 101 (2008) 1214–1222.
- [5] L.F. Pease, M. Sorci, S. Guha, D.H. Tsai, M.R. Zachariah, M.J. Tarlov, G. Belfort, *Biophys. J.* 99 (2010) 3979–3985.
- [6] M. Crona, C. Moffart, N.C. Friedrich, A. Hofer, *Nucleic Acids Res.* 39 (2011) 1381–1389.
- [7] E.A. Kapellios, S. Karamanou, S.A. Pergantis, *Anal. Bioanal. Chem.* 399 (2011) 2421–2433.
- [8] J.A. Loo, B. Berhane, C.S. Kaddis, K.M. Wooding, Y. Xie, S.L. Kaufman, I.V. Chernushevich, *J. Am. Soc. Mass Spectrom.* 16 (2005) 998–1008.
- [9] E.O. Knutson, K.T. Whitby, *J. Aerosol Sci.* 6 (1975) 443–451.
- [10] S.H. Kim, K.S. Woo, B.Y.H. Liu, M.R. Zachariah, *J. Colloid Interf. Sci.* 282 (2005) 46–57.
- [11] TSI Inc, Model 3025A Ultrafine Condensation Particle Counter Instruction Manual, 2005.
- [12] D.H. Tsai, L.F. Pease, R.A. Zangmeister, M.J. Tarlov, M.R. Zachariah, *Langmuir* 25 (2009) 140–146.
- [13] D.T. Kim, H.W. Blanch, C.J. Radke, *Langmuir* 18 (2002) 5841–5850.
- [14] T.J. McMaster, M.J. Miles, P.R. Shewry, A.S. Tatham, *Langmuir* 16 (2000) 1463–1468.
- [15] P.A. Mulheran, D. Pellenc, R.A. Bennett, R.J. Green, M. Sperrin, *Phys. Rev. Lett.* 100 (2008) 068102(1)–068102(4).
- [16] S. Guha, J.R. Wayment, M.D. Li, M.J. Tarlov, M.R. Zachariah, *Langmuir* 27 (2011) 13008–13014.
- [17] Y.L. Jeyachandran, J.A. Mielczarski, E. Mielczarski, B. Rai, *J. Colloid Interf. Sci.* 341 (2010) 136–142.
- [18] E.A. Scott, M.D. Nichols, L.H. Cordova, B.J. George, Y.S. Jun, D.L. Elbert, *Biomaterials* 29 (2008) 4481–4493.
- [19] S. Taylor, S. Smith, B. Windle, A. Guiseppi-Elie, *Nucleic Acids Res.* 31 (2003) 1–19.
- [20] L.A. Tessler, J.G. Reifengerger, R.D. Mitra, *Anal. Chem.* 81 (2009) 7141–7148.
- [21] M. Yue, J.C. Stachowiak, H. Lin, R. Datar, R. Cote, A. Majumdar, *Nano Lett.* 8 (2008) 520–524.
- [22] Y. Lin, Z.H. Su, *J. Polymer Sci., Part B – Polym. Phys.* 46 (2008) 1252–1257.
- [23] Y. Lin, X.S. Chen, X.B. Jing, Y.S. Jiang, Z.H. Su, *J. Appl. Polym. Sci.* 109 (2008) 530–536.
- [24] P. Kebarle, M. Peschke, *Anal. Chim. Acta* 406 (2000) 11–35.
- [25] S. Guha, L.F. Pease, K.A. Brorson, M.J. Tarlov, M.R. Zachariah, *J. Virol. Methods* (2011) 201–208.
- [26] D.H. Tsai, R.A. Zangmeister, L.F. Pease, M.J. Tarlov, M.R. Zachariah, *Langmuir* 24 (2008) 8483–8490.
- [27] A.A. Lall, X.F. Ma, S. Guha, G.W. Mulholland, M.R. Zachariah, *Aerosol Sci. Technol.* 42 (2009) 1075–1083.
- [28] M.D. Li, S. Guha, R.A. Zangmeister, M.J. Tarlov, M.R. Zachariah, *Aerosol Sci. Technol.* 45 (2011) 849–860.
- [29] M.D. Li, S. Guha, R.A. Zangmeister, M.J. Tarlov, M.R. Zachariah, *Langmuir* 27 (2011) 14732–14739.
- [30] R.J. Yon, *Biochem. J.* 126 (1972) 765–767.
- [31] T. Matsuda, H. Takano, K. Hayashi, Y. Taenaka, S. Takaichi, M. Umez, T. Nakamura, et al., *Am. Soc. Artif. Int. Organs* 30 (1984) 353–358.
- [32] A.V. Elgersma, R.L.J. Zsom, W. Norde, J. Lyklema, *J. Colloid Interf. Sci.* 138 (1990) 145–156.
- [33] C.E. Giacomelli, W. Norde, *J. Colloid Interf. Sci.* 233 (2001) 234–240.
- [34] A. Kondo, F. Murakami, K. Higashitani, *Biotech. Bioeng.* 40 (1992) 889–894.
- [35] H. Larsericsdotter, S. Oscarsson, J. Buijs, *J. Colloid Interf. Sci.* 289 (2005) 26–35.
- [36] S.J. McClellan, E.I. Franses, *Colloid Surf. A* 260 (2005) 265–275.
- [37] A. Kamyshny, O. Toledano, S. Magdassi, *Colloids Surf. B: Biointerfaces* 13 (1999) 187–194.
- [38] H.G. Curme, C.C. Natale, *J. Phys. Chem.* 68 (1964) 3009–3016.
- [39] Y. Kamiyama, J. Israelachvili, *Macromolecules* 25 (1992) 5081–5088.
- [40] T.J. Maternaghan, O.B. Bangham, R.H. Ottewill, *J. Photogr. Sci.* 28 (1980) 1–14.
- [41] K.A. Vaynberg, N.J. Wagner, R. Sharma, P. Martic, *J. Colloid Interf. Sci.* 205 (1998) 131–140.
- [42] K. Nakanishi, T. Sakiyama, K. Imamura, *J. Biosci. Bioeng.* 91 (2001) 233–244.
- [43] W. Norde, J.P. Favier, *Colloids Surf.* 64 (1992) 87–93.
- [44] M. van der Veen, M.C. Stuart, W. Norde, *Colloids Surf. B* 54 (2007) 136–142.
- [45] J.M. Johlin, *Proc. Soc. Expt. Bio. Med.* 26 (1929) 702–704.
- [46] N. Kawanishi, H.K. Christenson, B.W. Ninham, *J. Phys. Chem.* 94 (1990) 4611–4617.
- [47] J. Buijs, *J. Colloid Interf. Sci.* 178 (1996) 594–605.
- [48] T.T. Razunguzwa, M. Warriar, A.T. Timperman, *Anal. Chem.* 78 (2006) 4326–4333.